Characterising the influence of milk fat towards an application for extrusion-based 3D-printing of casein−whey protein suspensions via the pH−temperature-route

Daffner, Kilian; Ong, Lydia; Hanssen, Eric; Gras, Sally; Mills, Tom

DOI:
10.1016/j.foodhyd.2021.106642

Journal of Food Hydrocolloids

Characterising the influence of milk fat towards an application for extrusion-based 3D-printing of casein−whey protein suspensions via the pH−temperature-route

Kilian Daffner [a], Lydia Ong [b,c], Eric Hanssen [d,e], Sally Gras [b,c,e], Tom Mills [a]

[a] Department of Chemical Engineering, University of Birmingham, Edgbaston, Birmingham B15 2TT, United Kingdom

[b] The ARC Dairy Innovation Hub, The University of Melbourne, Parkville, Victoria, 3110, Australia

[c] Department of Chemical Engineering, The University of Melbourne, Parkville, Victoria, 3010, Australia

[d] Advanced Microscopy Facility, The Bio21 Molecular Science and Biotechnology Institute, The University of Melbourne, Parkville, Victoria, 3010, Australia

[e] Department of Biochemistry and Molecular Biology, The University of Melbourne, Parkville, Victoria, 3010, Australia

Corresponding author: Kilian Daffner

E-mail address: KXD744@bham.ac.uk

Keywords: food printing, acidified milk gels, protein−fat suspension, heat-induced gelation, physical properties

A B S T R A C T

This study presents the design and characterisation of casein−whey protein suspensions (8.0/10.0% (w/w) casein and 2.0/2.5% (w/w) whey protein) mixed with dairy fat (1.0, 2.5 and 5.0% (w/w) total fat) processed via the pH−temperature-route in preparation for 3D-printing. Mechanical treatment was applied to significantly decrease the particle size of the milk fat globules and increase surface area, creating small fat globules (< 1 μm) covered with proteins, which could act as pseudo protein particles during gelation. Different proteins covered the fat globule surface after mechanical treatment, as a result of differences in the pH adjusted just prior to heating (6.55, 6.9 or 7.1). The protein-fat suspensions appeared similar by transmission electron cryogenic microscopy and the zeta-potential of all particles was unchanged by the heating pH, with a similar charge to the solution (~ −20 mV) occurring after acidification (pH 4.8/5.0) at low temperatures (2°C). A low heating pH (6.55) resulted in increased sol−gel transition temperatures (G′ = 1 Pa) and a decreased rate of aggregation for protein−fat suspensions. A higher heating pH (6.9 and 7.1) caused an increased rate of aggregation (aggregation rate ≥ 250 Pa/ 10 K), resulting in materials more promising for application in extrusion-based printing. 3D-printing of formulations into small rectangles, inclusive of a sol−gel transition in a heated nozzle, was conducted to relate the aggregation rate towards printability.

1 Introduction

3D-printing, or additive manufacturing (AM), is a robotic construction technology that deposits materials layer-by-layer to build a three-dimensional object and that gains more and more interest in the area of foods (Wegrzyn, Golding, & Archer, 2012). 3D-printing of food, or food layered manufacturing (FLM), has been recently used to print a different range of food grade materials, including chocolate (Lanaro et al., 2017), hydrocolloid-based materials (Gholamipour-Shirazi et al., 2019) or processed cheese (Le Tohic et al., 2017), although the first food being printed was already in 2006 (Malone & Lipson, 2006). This printing technology offers advantages such as individualised products, flexibility with respect to nutritional content, and also the potential to reduce waste and storage or distribution costs of the final product compared to conventional mass production of food (Godoi, Prakash, & Bhandari, 2016; Ross, Kelly, & Crowley, 2019).

While the actual printing of food and post-characterisation following printing has received considerable attention, few experiments have considered defining the desirable material properties for optimal printing (Derossi, Caporizzi, Azzollini, & Severini, 2018). Food grade materials have complex nano- and microstructure, as well as altered properties associated with solid to liquid phase transition, complicating their use in printing. A greater understanding of the material properties will enable the design of useful formulations and is perhaps of one the most important steps in the printing of a range of edible foods. Edible and printable formulations need to match several requirements. For example, they should ideally be of homogenous composition, have suitable flow properties and enable printability in a layer-by-layer manner (Godoi et al., 2016; Kim, Bae, & Park, 2017).

There is a high demand for fermented concentrated dairy products, rich in protein and fat, such as Greek yogurt or fresh cheese (Jørgensen et al., 2019), and FLM has the potential to produce dairy-based products for tailored nutrition. Nöbel, Seifert, Schäfer, Daffner and Hinrichs (2018)

66 were the first to implement a pH−temperature (T)-route, including cold acidification followed
67 by heating, for printing of milk concentrates inclusive of a sol−gel transition, which resulted in
68 small printed spheres. For the pH−T-route, direct acidification at cold temperatures (≤ 10°C) to
69 pH values approaching the isoelectric point (IEP) of casein (4.6) helped to maintain solution
70 (sol)−characteristics due to a reduction of hydrophobic interaction forces (Horne, 1998). In-
71 creased temperatures then resulted in increasing hydrophobic interaction forces and particle
72 aggregation (Hammelehle, 1994; Roefs, 1986; Schäfer et al., 2018). Pre-chilled acidified con-
73 centrates from milk microfiltration differing in pH (4.8 – 5.4) and casein content (8.0 – 12.0%
74 (w/w)) have also been investigated and characterised for their suitability for 3D-printing (Nöbel
75 et al., 2018; Nöbel, Seifert, Schäfer, Daffner, & Hinrichs, 2020). Formulations at pH 4.8 formed
76 firm and homogeneous milk gels when printed. In contrast, the milk gels at pH 5.0 were not
77 mechanically stable after printing, illustrating the importance of pH as a process variable to
78 alter printed food properties.

79 Recently, casein−whey protein suspensions differing in their protein content, acidification - and
80 the pH at which heating was conducted were also characterised via the pH−T-route (Daffner et
81 al., 2020a). It would be of high interest to see whether dairy fat could be added to such formu-
82 lations and how this would change the microstructure and suitability of the dairy-based feed-
83 stock regarding printing. It is established that the rheological behaviour of dairy products like
84 cheese, yoghurt or mayonnaise is influenced by the presence of emulsified fat (Dickinson,
85 2012). Mechanical input causes oil droplets being covered and stabilised by a thin layer of
86 proteins adsorbed at the oil−water interface (Dickinson, 1994). During high pressure homoge-
87 nisation, CM and casein molecules also adsorb at the surface of the newly created milk fat
88 globule membrane (MFGM), sterically and electrostatically stabilising the droplets against re-
89 coalescence (McClements, 2004). Homogenisation has also been shown to cause milk fat glob-
90 ules (MFG) to behave to some extent like CM (Buchheim, 1986).

The surface properties are a further characteristic of the MFG that can influence printability. The zeta (ζ)-potential of MFG is reported to be around −13.5 mV (Michalski, Michel, Sainmont, & Briard, 2002a), with the MFGM phospholipids having a similar potential of −13 mV (Liu, Ye, Liu, Liu, & Singh, 2013). This ζ-potential increases to around −20 mV for homogenised MFG due to CM covering the newly created surface, approaching the ζ-potential of the protein casein. These results led to the assumption that the electrophoretic mobility of casein in the serum and casein adsorbed on the surface of the MFG were the same (Michalski et al., 2002a). When included in dairy gels, the MFG with a surface covered by casein and whey protein causes an increase in firmness, essentially increasing the apparent protein concentration (Aguilera & Kessler, 1988; Hammelehle, 1994; Ji et al. 2016; Van Vliet & Dentener-Kikkert, 1982).

MFG with protein on the surface were shown to act as pseudo-protein particles during gelation and increase gel firmness (Ji, Lee, & Anema, 2016). The aim of this study was to develop novel printable formulations for tailored nutrition by adding dairy fat to casein−whey protein suspensions for application in extrusion-based FLM via the pH−T-route. Adjusting the pH before heating was expected to cause a change in the types of protein covering the surface of the MFG after mechanical input. We hypothesise that this change in the surface properties of the MFG influences the overall formulation characteristics, tailoring the sol−gel transition temperature and manipulating the aggregation rate, with the latter property recently related towards printability (Daffner et al., 2020a). Several parameters including the protein and the fat content, as well as the pH during heating and cold acidification, were adjusted to design and characterise novel formulations towards printing applications.

112 # 2 Material and Methods

113 ## 2.1 Material

114 Micellar casein concentrate (MCC 85) and German Prot 9000 - Whey protein isolate (WPI)
115 were provided by Sachsenmilch Milk & Whey Ingredients (Sachsenmilch Leppersdorf GmbH,
116 Wachau, Germany). The manufacturer specifications are provided in Daffner et al. (2020a).
117 Cream (dairy fat) was bought from a local supermarket (Sainsbury's, Birmingham, UK) and
118 100 mL contained 47.5% (w/w) fat, 1.5% (w/w) lactose, 1.5% (w/w) protein and 0.05% (w/w)
119 salt. For pH adjustment, citric acid (1M) (Sigma Aldrich, UK) was prepared in Milli-Q water
120 (Elix® 5 distillation apparatus, Millipore®, USA) and sodium hydroxide (1M) was bought from
121 Sigma Aldrich (UK).

122 ## 2.2 Sample preparation

123 Casein−whey protein suspensions (4:1 ratio, casein to whey protein) were prepared following
124 the procedure of Daffner et al. (2020a). After a full hydration of the proteins overnight, fat was
125 added to the protein suspensions (with a starting pH of 6.7 ± 0.1) to obtain final fat concentra-
126 tions of 1.0, 2.5 or 5.0% (w/w). Before the heat treatment, the pH was adjusted to 6.55 (with 1
127 M citric acid) or either 6.9 or 7.1 (with 1 M NaOH). The protein−fat suspensions were indirectly
128 heated in a water bath on a stirring plate at 80°C for 10 min to ensure denaturation of the whey
129 proteins (degree of denaturation $_{\beta\text{-LG}} \geq 80\%$; estimated from Kessler, 2002). After heating, the
130 protein−fat suspensions were subjected to pre-homogenisation at 50.0 ± 2.0°C using a high
131 intensity ultrasonic vibracell processor (Vibra Cell 750, Sonics, USA) operating in a continuous
132 mode, at 750 W and 20 kHz. The power output was set at 95% of the nominal power and
133 sonication was conducted for 2 min, with 4 seconds on and 2 seconds off (3 min in total).
134 Directly after pre-homogenisation, each sample was passed through a high-pressure valve ho-
135 mogeniser (Panda NS1001L-2K, Gea Niro Soavi, Parma, Italy) at 500 bars and 50.0 ± 2.0°C.
136 All formulations were cold acidified at 2°C to pH values of 4.8 or 5.0, as described in Daffner
137 et al. (2020a).

138 **2.3 Rheology**

139 Rheological measurements were conducted by a Kinexus Pro rheometer (Malvern Instruments,
140 UK) with a cup (D = 27.17 mm, depth = 63.5) and vane (d = 61 mm, height = 25 mm)-geometry.
141 For dynamic oscillatory measurements, temperature sweeps were performed from 2 – 60°C
142 with a heating rate of 1 K/min, following the procedure of Daffner et al. (2020a). The sol−gel
143 transition temperature was determined when G′ reached a value of 1 Pa (Daffner et al., 2020a;
144 Nöbel et al., 2018; Nöbel et al., 2020; Schäfer et al., 2018).

145 **2.4 Zeta-potential and particle size measurements**

146 The particle size and the zeta (ζ)-potential were determined using a Mastersizer 2000 (Malvern
147 Instruments, UK) and a Zetasizer (Malvern Instruments, UK). A drop of the untreated dairy fat
148 was placed into the circulating cell which contained deionised water and the particles in the
149 micro range were measured at 20°C. Refraction indices of 1.46 and 1.33 were set for milk fat
150 and water respectively. After homogenisation, the Zetasizer was used to characterise the for-
151 mulations to give particle size distribution in the nanometre range. Samples were diluted
152 100 times with deionised water before experiments and ζ-potential measurements were per-
153 formed over a range of pH values (6.8 to 4.8), as described in Daffner et al. (2020a).

154 **2.5 Microscopy**

155 **2.5.1 CLSM**

156 **2.5.1.1 Preparation of samples**

157 Thermally and mechanically treated protein−fat suspensions were prepared for CLSM, mainly
158 following the procedure of Ong, Dagastine, Kentish, & Gras (2010a). A volume of 10 µl of
159 each of fast green FCF solution (1 mg/ml in MilliQ water, Sigma-Aldrich, St. Louis, U.S.A.)
160 and Nile red solution (1 mg/ml in 100% dimethyl sulfoxide, Sigma-Aldrich, St. Louis, U.S.A.)
161 was added to 480 µl of the sample that included protein and fat particles. The stained sample
162 was diluted 1:5 with agarose solution (40°C, 0.25g/50 ml Milli Q water) to reduce particle

163 movement due to Brownian motion, as shown in previous literature (Lopez, Madec, & Jimenez-
164 Flores, 2010; Devnani, Ong., Kentish, & Gras, 2020). The fat specific stain Nile red only stained
165 the fat core of the MFG and did not provide any information about the MFGM (Ong et al.,
166 2010a). According to the procedure of Ong et al. (2010a), a 10 µl aliquot of the stained sample
167 was transferred to a cavity slide (0.7 mm in depth) (ProSciTech, Thuringowa, Australia), cov-
168 ered with a glass coverslip (0.17 mm thick) and secured with nail polish (Maybelline LLC,
169 U.S.A.). The sample was then inverted for analysis by CLSM.

170 **2.5.1.2 CLSM**

171 The microstructure of the samples was observed using an inverted confocal scanning laser mi-
172 croscope (Leica SP8; Leica Microsystems, Heidelberg, Germany) powered by Ar/Kr and He/Ne
173 lasers. All samples were viewed using an oil immersion 63 x lens (1.32 Numerical Aperture)
174 and the pinhole diameter was maintained at 1 Airy Unit. All the wavelengths were adjusted
175 according to Ong et al. (2010a).

176 **2.5.1.3 Image analysis of CLSM micrographs**

177 Image analysis of CLSM micrographs was performed with LAS X software (LAS X Core Of-
178 fline version for Life Science, Leica Microsystems). Images were restored by a deconvolution
179 process conducted with Huygens Essential 3.7 software (Scientific Volume Imaging, Nether-
180 lands).

181 **2.5.2 Cryogenic transmission electron microscopy and image analysis**

182 Thermally (80°C, 10 min; adjusted pH 6.55/ 6.9/ 7.1) and mechanically (sonication and homog-
183 enisation) treated protein−fat suspensions were prepared for cryo-EM, following the protocol
184 of Daffner et al. (2020b). Samples were diluted 1:10 with deionised water to ensure an optimal
185 number of particles for imaging. Next, a Formvar lacey carbon film mounted on a 300 mesh
186 copper grids (ProSciTech, Australia) was glow discharged to have a hydrophilic support on
187 which the samples (3 µl) were adsorbed. To freeze the sample the grids were then plunged in

188 liquid ethane using a Vitrobot (FEI Company, Eindhoven, Netherlands). The grids were ob-
189 served on a Tecnai G2 F30 (FEI Company, Eindhoven, Netherlands) operating at 200 kV with
190 no objective aperture, equipped with a CETA CMOS 4kx4k detector (FEI company, Eindho-
191 ven, Netherlands). A series of micrographs of increasing dose was recorded for all samples with
192 a defocus value of −6.66 µm. High pass filtering and differentiation of the fat and protein par-
193 ticles was performed as described in Daffner et al. (2020b).

194 **2.6 SDS-PAGE**

195 **2.6.1 Separation and washing of the MFG surface proteins**

196 The proteins on the surface of the MFG after thermal and mechanical treatment were analysed
197 via SDS-PAGE following the isolation procedure of Sharma, Singh, & Taylor (1996a/ 1996b)
198 and Ye, Singh, Taylor, & Anema (2002), with a few changes. This procedure involved centrif-
199 ugation (Thermo Sorvall RC-6-Plus; Thermo Scientific, Asheville, USA) of the samples to re-
200 cover the cream layer first, followed by a washing step to remove serum proteins, and determi-
201 nation of the different types of casein and whey protein covering the fat globule surface layer
202 (Sharma & Dalgleish, 1993). To increase the difference in the density between fat and serum
203 phase, 8.6 g of sucrose was added per 30 g of sample, followed by centrifugation at 18.000 g
204 for 20 min at 20°C to separate the cream. After decanting the supernatant containing excess
205 proteins in solution, not bound to the fat globule membrane, the cream layer at the top of the
206 sample was washed with deionised water and centrifuged at 18.000 g for 20 min at 20°C to
207 remove any further unbound proteins. The washing step was repeated two times, as no further
208 changes in protein content were found when monitoring the supernatant with SDS-PAGE.

209 **2.6.2 Isolation and analysis of the fat globule surface protein components**

210 The identity of the proteins covering the MFG was determined with SDS-PAGE, using precast
211 Bis-Tris 4 – 12/ 12% polyacrylamide gels (Invitrogen, Mulgrave, Victoria, Australia). The

212 washed cream layers were dispersed (1:25) in a buffer (0.5 M Tris, 2% SDS, 0.5% β-mercap-
213 toethanol, pH adjusted to 6.8) to displace the protein from the FGM (Sharma et al., 1996a).
214 Samples were heated at 90°C for 5 min and centrifuged (2500 g, 20 min, 20°C) to remove the
215 fat from the sample. Subnatants (10 µl) were mixed with 5 µl NUPAGE 4x LDS sample buffer,
216 2 µl NUPAGE 10x reducing agent containing 0.5 M DTT and 5 µl β-mercaptoethanol. Samples
217 were heated (100°C, 3 min) and 10 µl of each sample was loaded into the gels. The gels were
218 run, stained, de-stained and visualised as described in Daffner et al. (2020a).

219 **2.7 Set-up of a customised 3D-printer**

220 The retrofitted set-up described in Daffner et al. (2020a) was used for extrusion-based 3D-
221 printing of small rectangles (25 x 25 x 3 mm; 3 layers above each other). A commercially
222 available plastic printer (Creality Ender 3 Printer; Creality, Shenzhen, China) was customised
223 and used. Before the printing process, the syringe was loaded with 60 ml of the cold acidified
224 protein−fat suspension. To maintain sol−characteristics, a temperature of 2°C was maintained
225 within the syringe cooling jacket. For the formulations to be printed, we followed the tempera-
226 ture-time profiles from another of our previous papers (Nöbel et al., 2020). The temperature of
227 the feedstock before the nozzle was adjusted as follows: $T_{sol-gel}$ −5K to avoid pre−gelation of
228 the formulations and to ensure a heat-triggered sol−gel transition within the length of the nozzle.
229 Materials were transported via a pipe to the copper nozzle (plastic dye at the end, 1.15 mm in
230 diameter), heated with the heating element and a sol−gel transition was induced. The printing
231 bed was not heated or cooled in this set-up. Printing was performed on a hydrophobic printing
232 paper (10 x 10 cm; Legamaster International B.V., The Netherlands) to prevent spreading of
233 the first layer.

234 **2.8 Statistics**

235 The data plotted in the publication includes the average of at least three measurements accom-
236 panied by error bars that consist of the standard deviation of the mean. In the case where mean

237 values of an observation are compared between samples the data have been subjected to analy-
238 sis of variance (ANOVA) in order to determine significant differences. Data analysis was con-
239 ducted with Sigma Plot 12.5 (Systat Software Inc., San Jose, CA, USA). Individual samples
240 were compared with Student's t-test and a level of significance of $p < 0.05$ was chosen.

241 3 Results

242 3.1 Physico-chemical characterisation of the sol-state

243 The pH−T-route was selected for the creation of promising protein-based formulations with
244 added dairy fat for extrusion-based 3D-printing. Mechanical damage of the MFG in the prepa-
245 ration is necessary to decrease the size and to cover the increased surface area of the MFG with
246 proteins. Previous studies have shown casein and whey proteins to cover more than 40% of the
247 newly created secondary milk fat globule membrane (SFGM), resulting in a significant increase
248 in the storage modulus G′, shown for acid- and rennet-induced milk gels (Michalski, Cariou,
249 Michel, & Garnier, 2002b). Better gel properties were achieved, if the heating step, which de-
250 natures whey proteins, was conducted before the homogenisation step (Hammelehle, 1994),
251 allowing the denatured whey proteins to interact with the MFG, as well as with CM, increasing
252 the number of particles contributing to the overall gelation process.

253 The goal of this study was to identify if those smaller MFG could behave like CM and actively
254 contribute to the protein-based gelation process as structure promoters (Buchheim, 1986; Ji et
255 al., 2016; Michalski, Michel, & Geneste, 2002c), thereby enhancing printability. The particle
256 size, zeta-potential and surface coverage of the newly created secondary milk fat globule mem-
257 brane (SDS-PAGE, microscopy), sol−gel transition temperature and aggregation kinetics were
258 investigated, building on a prior study of protein-based systems (Daffner et al., 2020a).

3.1.1 Zeta-potential and surface characteristics

Casein−whey protein suspensions were mixed with fat and heated at different pH, treated by mechanical input and then cooled to 2°C, followed by acidification. The ζ-potential of the resulting samples is shown in *Fig. 1*, where the data represents an average of all protein and fat particles captured within the sample. An almost linear increase of the ζ-potential was found with decreasing pH during acidification and this trend was independent of the pH value before heating. A non-heated micellar casein suspension without any whey protein and fat was also included for comparison (Daffner et al., 2020a).

At an acidification pH of 4.8 and 5.0, the ζ-potential of casein−whey protein suspensions with fat was around −20 mV. This demonstrated that sol-characteristics of all formulations, independent of the heating pH, were maintained at an acidification temperature of 2°C and electrostatic repulsion forces between particles were dominant.

A slight trend to lower ζ-potential values with increasing heating pH was found. Compared to the pure micellar casein suspensions (non-heated), the addition of fat caused a significant increase in the magnitude of the ζ-potential, similar to previous observations (Daffner et al., 2020a). This could be explained by the coverage of the MFG surface with a more complex range of proteins, including CM, κ-casein−whey protein complexes or denatured whey protein (-aggregates) as a result of the pre-processing treatments applied here.

A lower ζ-potential between −17 mV to −13 mV was found for MFG in whole milk after homogenisation, dependent on the Ca^{2+} concentration (Dalgleish, 1984). For MFG covered with CM after homogenisation at 500 bar, Michalski et al. (2002a) found a similar ζ-potential of −20 mV, compared to −13.5 mV for the native MFG. The ζ-potential of MFG increased with increasing homogenisation pressure, due to the production of smaller MFG and an increase in surface area covered with more CM. Within their research, they concluded that the ζ-potential of a free protein and that of protein adsorbed on a fat globule surface were the same. It was

284 assumed that the protein charged molecular protuberances on the surface of the carrier were
285 responsible for the mobility of the particles rather than the carrier size (Rajagopalan & Hie-
286 menz, 1997).

287 **3.1.2 Particle size distribution**

288 The influence of a mechanical input on the particle size distribution of casein−whey protein
289 suspensions with three different fat contents (1.0% (w/w), 2.5% (w/w) and 5.0% (w/w)) after
290 heating at different pH (6.55, 6.9 and 7.1) is illustrated in *Fig. 2*. The sonication step, followed
291 by high pressure homogenisation caused a significant decrease in the particle size and resulted
292 in a monomodal particle size distribution, with no changes found dependent on the pH at which
293 heating was conducted. The addition of different amounts of fat to protein suspensions had no
294 significant effect on the particle size distribution, although there was a slight tendency to bigger
295 particles with increasing fat content. The z-average of all the particles captured within the pro-
296 tein−fat suspensions was 275 nm (*Fig. 2 inset*), demonstrating a significant increase of 40 – 50
297 nm in the particle size compared to casein−whey protein suspensions with the same heating pH
298 but without any addition of fat (Daffner et al., 2020a). This larger size results from the fat
299 particles being larger than the protein particles, even after homogenisation.

300 To intentionally induce a fast, local and irreversible sol−gel transition during printing, the par-
301 ticles need to be within a certain size range; this ensures they will move sufficiently fast to
302 successfully collide and aggregate via the pH−T-route (Daffner et al., 2020a; Nöbel et al., 2018;
303 Nöbel et al., 2020). Formulations with no heat- and mechanical treatment contained large, na-
304 tive and emulsified MFG in the protein suspensions (see *Supplementary Fig. 1*), which slowed
305 down the aggregation and gelation of proteins (data not shown). It is expected that as the size
306 of the MFG approaches the size of the CM, there will be a higher chance that these particles
307 will behave in a similar way (Hammelehle, 1994). It is well known that the rheology of the

308 overall formulations depends on the behaviour of the continuous phase, if the dispersed parti-
309 cles are well separated from each other and do not aggregate (Dickinson, 1998). In this case,
310 the protein suspension will behave as desired if the MFG are sufficiently small and do not
311 associate.

312 **3.1.3 Micrographs from microscopy**

313 **3.1.3.1 CLSM**

314 CLSM was used to investigate the microstructure of casein−whey protein suspensions mixed
315 with dairy fat after a thermal and mechanical treatment (*Fig. 3*, after heating at pH 7.1) using
316 an intermediate final fat content of 2.5% (w/w). A homogenous distribution of the MFG could
317 be observed in all samples, regardless of the pH adjustment made prior to heating and a repre-
318 sentative CLSM image at pH 7.1 is presented in *Fig. 3*. The MFG, stained red in these images,
319 were distributed relatively evenly between the proteins, which were stained green, with the
320 unstained serum phase appearing black in these images. The size of the MFG, which ranges
321 from 50 nm – 1000 nm was consistent with the size of ~275 nm observed by light scattering
322 (*Figure 2*). Protein particles were also found to be adsorbed on the surface of MFG, where they
323 appear as green particles.

324 Independent of the heating pH, the MFG featured proteins interacting with the membrane sur-
325 face. After image deconvolution and digital magnification, the proteins covering the surface of
326 the MFG could be better observed (*Fig. 3*, right). Nevertheless, no detailed information of the
327 specific type of protein, protein subunits or aggregates covering the MFG surface could be
328 obtained with this standard confocal microscopy due to the resolution limit of this technique.

329 **3.1.3.2 Cryogenic-EM**

330 A novel technique was recently described for the more detailed visualisation of interactions be-
331 tween the MFG and the proteins in the hydrated state without chemical fixatives or embedding

332 (Daffner et al., 2020b). This method of different time-dependent radiation damage allows dif-
333 ferentiation between protein (visible damage > 150 $e^-/Å^2$) and fat (visible damage < 25 $e^-/Å^2$)
334 particles (Daffner et al., 2020b). Previous studies have observed that the mass of casein and
335 whey protein on the surface of MFG after mechanical and thermal input strongly depended on
336 several parameters including homogenisation pressure, heat treatment and casein-fat ratio (Wal-
337 stra & Jenness, 1984; Sharma & Dalgleish, 1993; Cano-Ruiz & Richter, 1997). The new cryo
338 technique was therefore applied to assess the presence of proteins on the surface of MFG after
339 the processing techniques applied here.

340 Proteins were observed on MFG after a heating step applied at different pH (pH 6.55, 6.9 or
341 7.1) and homogenisation. The images in *Fig. 4* show small spherical MFG (~ 100 nm) covered
342 with larger CM and smaller proteins. The proteins were distinguished by increasing the beam
343 exposure. Whilst the proteins were clearly present, no differences were observed in the appear-
344 ance of these structures for the samples with different heating pH (6.55, 6.9 or 7.1). This obser-
345 vation is consistent with the finding of intact CM covering the MFG surface under similar con-
346 ditions (heating at 79°C and a homogenisation pressure of 70 bar), Ye, Anema, & Singh (2008)
347 using the more traditional approach with fixed samples and TEM. The new cryo method is
348 useful for the determination of protein in the hydrated state but does not provide information of
349 the specific type of protein covering the MFG surface. The samples were therefore assessed
350 next by SDS-PAGE analysis.

351 **3.1.4 Analysis of the surface coverage of the MFG via SDS-PAGE**

352 The thermal and mechanical treatment applied in this study reduced the MFG size (see *Fig. 2*
353 and *Fig. 4*) and conversely increased the surface area, allowing proteins to absorb onto the
354 surface of the smaller MFG. An increase in the pH before heating from 6.55 to 7.1 potentially
355 altered proteins in the samples, without changing the MFG surface area, which may be expected
356 to alter protein composition on the MFG.

357 An increase in the pH at heating caused an increase in the proportions of α- and β-casein on the
358 surface of the MFG and only very faint bands of κ-casein and β-LG were detected adsorbed to
359 the surface under these conditions, as shown in *Fig. 5,* where the SDS-PAGE gel shows the
360 protein extracted from the MFG surface and the variation in proteins present for replicate ex-
361 tract samples. Both α_{s1}- and β-casein have a strong tendency to adsorb at hydrophobic surfaces,
362 due to accessible non-polar residues (Dickinson, 1999) and were expected to preferentially
363 cover the surface of the MFG compared to other proteins, as occurred for all conditions exam-
364 ined here. The increase in casein absorption as a function of pH at heating also lead to an in-
365 crease in the casein−whey protein ratio on the MFG surface from 6.6 to 14.7 as the heating pH
366 was increased, as shown in *Table 1.*

367 The dissociation of κ-casein from the CM at higher heating pH (6.9, 7.1) has been reported
368 previously (Anema & Klostermeyer, 1997; Daffner et al., 2020a), changing the characteristics
369 of the CM, as well as the aggregates found in the milk serum. This could explain for the pref-
370 erential adsorption of CM depleted of κ-casein and high in α- and β-casein observed in this
371 study. This dissociation was also confirmed at higher solids (up to 25%), with increasing
372 pH (6.5 – 7.1) and increasing concentrations causing an increase in the extent of κ-casein dis-
373 sociation (Singh & Creamer, 1991). For the same pure protein-based system, increasing the
374 heating pH to 6.9 or 7.1 caused increasing amounts of κ-casein dissociating from the CM into
375 the serum, resulting in κ-casein−whey protein complexes in the serum and decreased levels of

376 CM covered with whey proteins (Daffner et al., 2020a). For concentrated milk systems after a
377 heating step (120°C, 10 min), Singh & Creamer (1991) found that the dissociated protein was
378 composed of 70% κ-casein, 20% β-casein and 10% α-casein.

379 Other studies have not observed whey proteins on the surface of MFG, as occurred here, due to
380 the difference in processing conditions, highlighting the potential for protein composition to be
381 systematically altered. Only casein (α, β and κ) and no whey or native membrane proteins (e.g.
382 xanthinoxidase) were found on the surface of the MFG after homogenisation (Ong et al.,
383 2010a), potentially due to low heating temperatures and a lack of denaturation of the whey
384 proteins. Similarly, whey proteins were absent on the surface of the MFG after microfluidiza-
385 tion, if the temperature was less than 70°C (Sharma & Dalgleish (1993).

386 Other processing variables appear to have less effect on the composition of proteins adsorbed
387 to the MFG. Homogenisation pressure was found to have no effect on the composition of the
388 proteins on the surface of the MFG, with 70% of the material characterised as casein and the
389 rest being whey and native membrane proteins for all conditions examined (Cano-Ruiz & Rich-
390 ter, 1997). Sharma et al. (1996b) found the amount of κ-casein covering the surface of the MFG
391 independent of the heat treatment performed and the order of the heating and homogenisation
392 steps. They concluded that the deposition of κ-casein depended only on the homogenisation
393 step. The κ-casein−whey protein complexes in the serum and on the MFG surface were pro-
394 posed to be similar after heating and homogenisation (Sharma et al., 1996a).

395 Similar to the results of our work (compare *Table 1*), Sharma et al. (1996a) found increasing
396 amounts of α_s- and β-casein, but decreasing amounts of κ-casein and β-LG covering the surface
397 of MFG after mechanical input, if the pH before a heating step was adjusted from 6.3 to 7.3,
398 which also resulted in an increase in the casein to whey protein ratio from 4.62 (pH 6.3) to
399 8.01 (pH 7.3) on the surface of the MFG.

400 **3.2 Rheological characterisation of sol−gel transition**

401 The sol−gel transition temperatures ($T_{sol-gel}$) of all formulations were determined with temper-
402 ature sweeps at a heating rate of 1 K/min. The goal was to investigate the effect of additional
403 dairy fat on the rheological behaviour of the protein-based systems (Daffner et al., 2020a).
404 $T_{sol-gel}$ of cold acidified casein−whey protein suspensions (8.0% (w/w) CS, 2.0% (w/w) WP)
405 with added fat (to final fat contents of 1.0-, 2.5- and 5.0% (w/w)) after heating (pH 6.55, 6.9,
406 7.1) and mechanical input are shown in *Figure 6*. It was proposed that homogenised MFG can
407 mimic the behaviour of CM and potentially coagulate in a manner similar to CM (Ji et al., 2016;
408 Walstra & Jenness, 1984).

409 To enable comparison the behaviour of casein−whey protein suspensions without fat (Daffner
410 et al., 2020a) was added as a baseline to all figures. The sol area lies below this line and the gel
411 area above the line. The two most promising formulations using acidifications pH of 4.8 and
412 5.0, were chosen in the current study, based on previous studies (Daffner et al., 2020a; Nöbel
413 et al., 2018), which reported more promising characteristics, including higher aggregation rates
414 for these formulations, consistent with the desired application of 3D printing via the pH−T-
415 route.

416 $T_{sol-gel}$ of casein−whey protein suspensions with fat after heating at pH 6.55 are illustrated in
417 *Fig. 6 (A)*. Independent of the amount of fat, formulations showed lower values for the $T_{sol-gel}$
418 with decreasing pH value (4.8 compared to 5.0), which was in accordance with results for ca-
419 sein−whey protein suspensions (Daffner et al., 2020) and casein-based systems (Nöbel et al.,
420 2020). Apart from one sample (pH 5.0, 5.0% (w/w) fat content), higher $T_{sol-gel}$ (2 – 5°C) were
421 found. The more fat added, the closer the $T_{sol-gel}$ were to those of formulations without any
422 additional fat (*Fig. 6 (A)*). Increasing the heating pH (6.9) for formulations with fat resulted in
423 lower $T_{sol-gel}$ compared to results after a heating pH of 6.55 (*Fig. 6 (B)*). While 1.0- and 2.5%
424 (w/w) of fat caused a slight increase in the $T_{sol-gel}$, a tendency to decreased values with 5.0%

425 (w/w) fat was found, independent of the acidification pH, which could potentially be explained
426 with an increasing amount of particles per unit area capable to aggregate and form a gel.

427 The tendency to lower $T_{sol-gel}$ with increased heating pH for casein−whey protein formulations
428 with fat was further confirmed by results at a heating pH of 7.1. A decrease (2°C after addition
429 of 1.0- and 2.5% (w/w) fat and more than 4°C after addition of 5.0% (w/w) fat) of $T_{sol-gel}$ at an
430 acidification pH of 5.0 compared to the formulation without any fat added is illustrated in *Fig.*
431 *6 (C)*. If these formulations (heating pH 7.1) were acidified to pH 4.8, pre-gelation characteris-
432 tics ($G' > 1$ Pa, where particles already started to aggregate before any heat-induced gelation)
433 occurred, making them unsuitable for printing.

434 The decrease in $T_{sol-gel}$ at higher heating pH is likely due to changes of the protein composition
435 of the MFG membrane, shown via gel electrophoresis (compare *Fig. 5*). For acid gelation, 40%
436 of the membrane had to be coated by serum proteins to significantly increase the storage mod-
437 ulus (Michalski et al., 2002b). In contrast to the finding of Hammelehle (1994) who did not find
438 a shift in the coagulation after heating the formulations, our study showed significant changes
439 in the $T_{sol-gel}$ for protein-fat suspensions (8.0% (w/w) casein and 2.0% (w/w) whey protein),
440 strongly dependent on the heating pH.

441 The results for $T_{sol-gel}$ of formulations with 10.0% (w/w) casein and 2.5% (w/w) whey protein
442 with additional fat are shown in *Fig. 6 (D)*. Due to the increased amount of protein plus addi-
443 tional fat, the overall total solid content increased. As a result, fewer formulations could be
444 analysed and the results of formulations after a heating pH of 6.55 and 6.9 were summed up in
445 one figure, which resulted in two coagulation lines. Pre-gelation ($G' > 1$ Pa) was found for all
446 formulations with a heating pH of 7.1 and no further analysis was conducted. A slight tendency
447 to lower $T_{sol-gel}$ at both heating pH values (6.55 and 6.9) was found for all formulations.

448 At this higher protein content and the lower acidification pH values of 4.8 and 5.0, the influence
449 of additional fat on $T_{sol-gel}$ was less distinct compared to results with the lower protein content.

450 Pre-gelation characteristics (G′ > 1 Pa) were found for several formulations after the addition
451 of fat (e.g. pH 4.8, 5.0% (w/w) fat, heated pH 6.55 or pH 5.0, ≥ 2.5% (w/w) fat, heated pH 6.9),
452 explained with the increase in the total solid content and a higher amount of particles per unit
453 volume.

454 **3.3 Aggregation rate of casein−whey protein suspensions mixed with milk fat**

455 As described in Daffner et al. (2020a), the aggregation rate (represented by the evolution of the
456 G′ after reaching the sol−gel transition temperature) of the formulations was used to analyse the
457 aggregations kinetics of casein−whey protein suspensions mixed with fat. For a simplified com-
458 parison, a solid line was added in all images which represented the aggregation rate of pure
459 protein-based suspensions. The horizontal dashed line for the aggregation rate was used as a
460 positive indicator from printing tests towards future printing applications of casein−whey pro-
461 tein suspensions, if values of 250 Pa/ 10 K were exceeded (Daffner et al., 2020a).

462 The influence of three different amounts of fat on formulations with 8.0% (w/w) casein and
463 2.0% (w/w) whey protein followed by thermal (pH 6.55, 6.9 and 7.1) and mechanical energy
464 input is shown in *Fig. 7 (A-C)*. Increased values for the aggregation rate (storage modulus G′)
465 with decreasing acidification pH (5.0 to 4.8) were found for formulations after a heating step at
466 pH 6.55. If 1.0% (w/w) fat was added, independent of the acidification pH, the aggregation rate
467 significantly decreased (47.7% at pH 5.0 and 29.0% at pH 4.8) compared to formulations with-
468 out fat. While no change in G′ was found after the addition of 2.5% (w/w) fat at acidification
469 pH 4.8 and 5.0, the 5.0% (w/w) additional fat increased the values for the storage modulus G′,
470 with maximum values of around 300 Pa at pH 4.8. The formulations with 2.5 and 5.0% (w/w)
471 fat reached around 250 Pa/ 10 K for the aggregation rate and simple printing tests were con-
472 ducted. As shown in *Fig. 7* (A), a stable and firm 3D-printed gel was only found for the formu-
473 lation with 5.0% (w/w) fat at an acidification pH of 4.8, while the one at pH 5.0 (not shown)
474 could not maintain the rectangular shape.

475 The results for the aggregation rate of the formulations after an increased heating pH of 6.9 and
476 different amounts of fat added are illustrated in *Fig. 7 (B)*. The values for the storage modulus
477 G′ increased with decreasing acidification pH and increasingly amount of additional fat (one
478 exception at pH 5.0 and 1.0% (w/w) fat content, with the highest increase in G′ of 22.5% at pH
479 5.0 and 5.0% (w/w) fat. A significant increase of G′ (heating pH 6.9) compared to formulations
480 heated at lower pH (6.55) was demonstrated, evidenced by reaching or exceeding an aggrega-
481 tion rate of around 250 Pa/10 K for all formulations with milk fat addition. Although all formu-
482 lations with fat addition showed promising aggregation rates after being heated at pH 6.9, only
483 those acidified to pH 4.8 resulted in firm and very stable 3D-printed gels when heated during
484 conveying (see printed gels related to aggregation rate in *Fig. 7 (B)*).

485 At a slightly alkaline heating pH of 7.1 and after the addition of fat, fewer casein−whey protein
486 formulations could be analysed (see *Fig. 7 (C)*), as an acidification pH value of 4.8 resulted in
487 pre-gelation characteristics (G′ > 1 Pa), preventing a temperature-triggered sol−gel transition.
488 At an acidification pH of 5.0, a trend towards increased values of G′ in samples with 1.0 and
489 2.5% (w/w) fat content was found, which became significant in the sample with 5.0% (w/w) fat
490 content. All the formulations reached or exceeded an aggregation rate of 250 Pa/ 10 K with the
491 highest value of 325.9 Pa/ 10 K ± 18.3 Pa/ 10 K (5.0% (w/w) fat). Independent of the amount
492 of fat added, all three formulations, which were heated at pH 7.1 and cold acidified to pH 5.0,
493 could be printed into small rectangular gels (*Fig. 7 (C)*). A linear increase in the gel firmness
494 measured using penetration tests after addition of fat (2.0 – 10.0% (w/w) fat) to protein gels
495 (4.3% (w/w)), manufactured via the pH−T-route, was found previously (Hammelehle, 1994).
496 Such high fat contents could not be used in this study due to pre–gelation characteristics
497 (G′ > 1 Pa) when the fat content of the samples was higher than 5.0% (w/w).

498 The influence of the addition of 1.0 and 2.5% (w/w) fat on the aggregation rate of formulations
499 with an increased overall protein content of 12.5% (w/w), consisting of 10.0% (w/w) casein

500 and 2.5% (w/w) whey protein, followed by thermal (pH 6.55, 6.9) and mechanical input is
501 shown in *Fig. 7 (D)*. Due to pre-gelation (G′ > 1 Pa) after the addition of fat at the higher protein
502 content (total solid content increased), several samples could not be produced and no formula-
503 tions with a heating pH of 7.1 was further investigated. This included the formulation with a
504 heating pH of 6.55 and 5.0% (w/w) fat) which could not be further processed. The results of
505 the aggregation rate of formulations after both heating pH values were combined in one figure
506 (*Fig. 7 (D)*). At higher protein contents, a significant decrease in the storage modulus was
507 demonstrated for all formulations after the addition of fat, independent of the heating pH and
508 the acidification pH. This was proposed to be the result of the increased amount of total solids
509 (fat and protein) in the same unit volume compared to formulations without any additional fat,
510 therefore slowing down the aggregation kinetics of the protein particles, if an increase in the
511 temperature (pH–T-route) triggered collision and gelation of the particles. All three formula-
512 tions at this higher protein content were tested for printing and resulted in firm gels.

513 **3.4 Tailored casein micelle and MFG surface characteristics towards printing applica-**
514 **tions**

515 Having applied the same thermal treatment (80°C, 10 min), CM with different composition and
516 surface characteristics occurred, depending on the pH adjusted before heating to denature the
517 whey proteins (Daffner et al., 2020a). The CM and protein subunits/ aggregates, which covered
518 the MFG after thermal and mechanical treatment in this study, provided electrostatic and steric
519 repulsion forces hindering coalescence of the fat particles. The small changes in the pH adjusted
520 before heating allowed tailoring of the surface characteristics of the MFG, changing the sol−gel
521 transition temperature (*Fig. 6*) as well as the aggregation rate (*Fig. 7*) of the protein suspensions
522 mixed with fat compared to pure casein-whey protein based suspensions of our previous study
523 (Daffner et al., 2020a). Therefore, the pH sensitive CM as well as the MFG covered with pro-
524 teins reacted to changes in the acidification pH and contributed to the gelation process via the
525 pH−T-route. A schematic illustration (Fig. 8) shows the effect of heating (80°C, 10 min) at the

526 three adjusted pH values (6.55, 6.9, 7.1) and a mechanical input (sonication and homogenisation
527 at 500 bar) on the casein−whey protein suspensions mixed with dairy fat, as well as the pro-
528 posed interactions between proteins and fat globules. Walstra & Jenness (1984) found that MFG
529 after homogenisation could behave like CM and could be coagulated in the same way as pure
530 proteins, although their experiment was conducted under resting conditions. In this study, the
531 MFG, which were coated with different types of dairy proteins on the surface after mechanical
532 input, showed a similar behaviour.

533 During high pressure homogenisation, CM adsorb faster to droplet surfaces than individual ca-
534 sein molecules (McClements, 2004). Results of the SDS-PAGE (*Fig. 5*) showed that κ-depleted
535 CM (heating pH 7.1) covered the surface of MFG, which resulted in MFG more prone to ag-
536 gregation compared to MFG covered with protein (CM with whey protein on the surface) after
537 heating at pH 6.55, evidenced by lower $T_{sol-gel}$ (compare *Fig. 6 (C)* to *(A)*). This was proposed
538 to occur due to a decrease of the steric repulsion forces on the surface of the MFG covered with
539 depleted CM, as parts of κ-casein dissociated into the serum which resulted in a less dense hairy
540 layer protruding into the serum phase.

541 The different surface characteristics of the MFG after mechanical treatment changed the micro-
542 structure of protein-fat formulations. As the aggregation rate was used as a positive indicator
543 towards printability with simple printing tests, not all formulations exceeding 250 Pa/ 10 K
544 were found to result in firm and stable gels. We assume that MFG, which were heated at pH
545 6.55, were covered with CM, CM with whey protein on their surface as well as denatured whey
546 protein aggregates, as shown from SDS-PAGE (*Fig. 5*). Those MFG were proposed to have
547 stronger steric repulsion forces due to κ-casein on the outside of the CM, protruding into the
548 serum. On the other hand, increased heating pH values (6.9, 7.1) resulted in κ-depleted CM
549 which covered the MFG, demonstrated by a decrease of κ-casein found during SDS-PAGE
550 (*Fig. 5*). It is assumed that this decrease in the amount of κ-casein on the outside of the casein

551 micelles and on the surface of the MFG caused lower steric repulsion forces, shown by higher
552 aggregation rates of those formulations.

553 At a total protein content of 10.0% (w/w), consisting of 8.0% (w/w) casein and 2.0% (w/w)
554 whey protein, only one formulation with additional fat after a heating pH of 6.55 was found to
555 be printable. On the other hand, three formulations at each heating pH (6.9 and 7.1) could be
556 printed, although a lower acidification pH 4.8 was necessary at heating pH 6.9. As CM were
557 most depleted in κ-casein after being heated at pH 7.1 and therefore, steric repulsion forces of
558 CM on their own and on the surface of MFG decreased, those formulations were the only ones
559 being able to be printed at pH 5.0. The proposed interactions between protein and fat particles
560 depending on the heating pH were schematically illustrated in *Fig. 8*. A similar increase of
561 adsorbed caseins (α_s and β) with increasing heating pH value, but decreasing amounts of κ-
562 casein and β-lactoglobulin were found elsewhere (Sharma et al., 1996a).

563 **4 Conclusion**

564 The effect of dairy fat on casein−whey protein suspensions was characterised regarding the
565 potential use for extrusion-based 3D-printing applications via the pH–T-route. Small fat parti-
566 cles in the nano metre range were mechanically produced and covered with different protein
567 particles to mimic protein behavior during gelation. For promising formulations, sol–character-
568 istics after cold acidification (pH 4.8/5.0), independent of the heating pH but dependent on the
569 protein content, were evidenced by ζ-potential (~ –20 mV) and rheology (G′ = 0.1 Pa) and a
570 steep increase of G′ above 1 Pa (sol−gel transition temperature) was found.

571 For protein-fat formulations heated at a lower pH (6.55) followed by mechanical input, an in-
572 crease in the sol−gel transition temperature and a decrease in the aggregation rate, independent
573 of the amount of fat added, was found. In contrast, a higher heating pH caused similar (pH 6.9)
574 respectively lower (pH 7.1) sol−gel transition temperatures. For those higher heating pH values,

increased aggregation kinetics compared to casein−whey protein based suspensions without fat were found, resulting in more promising material characteristics (G′ ≥ 250 Pa/ 10 K) for printing purposes. Dairy fat could thus be added to casein−whey protein suspensions which were considered to be printable via the pH−T-route, if the thermal and mechanical treatments tailored the material properties accordingly. Extrusion-based 3D-printing of protein-fat formulations inclusive a sol−gel transition was found to be more favourable at higher heating pH values.

Acknowledgements

This work was supported by the Engineering and Physical Sciences Research Council [grant number EP/N024818/1]. This research was supported under Australian Research Council's Industrial Transformation Research Program (ITRP) funding scheme (project number IH120100005). The ARC Dairy Innovation Hub is a collaboration between The University of Melbourne, The University of Queensland and Dairy Innovation Australia Ltd. The authors would like to thank Ian Norton as well as Eddie Pelan for fruitful discussions and Adabelle Ong for help with the SDS-PAGE. The authors would like to thank The Bio21 Molecular Science & Biotechnology Institute at The University of Melbourne for access to equipment. Cryo EM was carried out at the Bio 21 Advanced Microscopy Facility, at The University of Melbourne. We acknowledge Unternehmensgruppe Theo Mueller for gifting the powders.

References

Aguilera, J. M., & Kessler, Hg. (1988). Physicochemical and rheological properties of milk-fat globules with modified membranes. Milchwissenschaft 43 (1988), 411-415.

Buchheim, W. (1986). Membranes of milk fat globules ultrastructural biochemical and technological aspects. Kieler Milchwirtschliche Forschungsberichte, 38, 227-246.

Cano-Ruiz, M. E., & Richter, R. L. (1997). Effect of homogenisation pressure on the milk fat globule membrane proteins. Journal of Dairy Science, 80(11), 2732-2739.

Cho, Y. H., Lucey, J. A., & Singh, H. (1999). Rheological properties of acid milk gels as affected by the nature of the fat globule surface material and heat treatment of milk. International Dairy Journal, 9(8), 537-545.

Daffner, K., Vadodaria, S., Ong, L., Nöbel, S., Gras, S., Norton, I., & Mills, T. (2020a). Design and characterization of casein-whey protein suspensions via the pH-temperature-route for application in extrusion-based 3D-Printing. Food Hydrocolloids, 105850.

Daffner, K., Hanssen, E., Norton, I. T., Mills, T., Ong, L., & Gras, G. L. (2020b). Imaging of dairy emulsions via a novel approach of cryogenic transmission electron microscopy using beam exposure. Soft Matter, 16(34), 7888-7892.

Dalgleish, D. G. (1984). Measurement of electrophoretic mobilities and zeta-potentials of particles from milk using laser Doppler electrophoresis. Journal of Dairy Research, 51(3), 425-438.

Derossi, A., Caporizzi, R., Azzollini, D., & Severini, C. (2018). Application of 3D printing for customized food. A case on the development of a fruit-based snack for children. Journal of Food Engineering, 220, 65-75.

Devnani, B., Ong, L., Kentish, S., & Gras, S. (2020). Heat induced denaturation, aggregation and gelation of almond proteins in skim and full fat almond milk. Food Chemistry, 126901.

Dickinson, E. (1994). Protein-stabilized emulsions. Journal of Food Engineering, 22, 59-74.

Dickinson, E. (1998). Rheology of emulsions - The relationship to structure and stability. In Modern aspects of emulsion science (pp. 145-174).

Dickinson, E. (1999). Caseins in emulsions: interfacial properties and interactions. International Dairy Journal, 9(3-6), 305-312.

Dickinson, E. (2012). Emulsion gels: The structuring of soft solids with protein-stabilized oil droplets. Food hydrocolloids, 28(1), 224-241.

Godoi, F. C., Prakash, S., & Bhandari, B. R. (2016). 3d printing technologies applied for food design: Status and prospects. Journal of Food Engineering, 179, 44-54.

Guinee, T. P., Gorry, C. B., O'Callaghan, D. J., O'Kennedy, B. T., O'Brie, N., & Fenelon, M. A. (1997). The effects of composition and some processing treatments on the rennet coagulation properties of milk. International Journal of Dairy Technology, 50(3), 99-106.

Hammelehle, B. (1994). Die Direktsaeuerung von Milch. Untersuchungen zur gezielten Einflussnahme auf Textur und Konsistenz gesaeurter Milchgel. PhD Thessis. Muenchen: Technische Universitaet Muenchen/ Weihenstephan.

Horne, D. S. (1998). Casein interactions: casting light on the black boxes, the structure in dairy products. International Dairy Journal, 8(3), 171-177.

Huppertz, T., & Kelly, A. L. (2006). Physical chemistry of milk fat globules. In Advanced Dairy Chemistry Volume 2 Lipids (pp. 173-212). Springer, Boston, MA.

Jacob, M., Schmidt, M., Jaros, D., & Rohm, H. (2011). Measurement of milk clotting activity by rotational viscometry. Journal of dairy research, 78(2), 191-195.

Ji, Y. R., Lee, S. K., & Anema, S. G. (2016). Characterisation of heat-set milk protein gels. International dairy journal, 54, 10-20.

Jørgensen, C. E., Abrahamsen, R. K., Rukke, E. O., Hoffmann, T. K., Johansen, A. G., & Skeie, S. B. (2019). Processing of high-protein yoghurt–A review. International Dairy Journal, 88, 42-59.

Kessler, H. G. (2002). Food and bio process engineering. Dairy Technology, 5th edition (Verlag A. Kessler, Munich, Germany).

Lanaro, M., Forrestal, D. P., Scheurer, S., Slinger, D. J., Liao, S., Powell, S. K., & Woodruff, M. A. (2017). 3D printing complex chocolate objects: Platform design, optimization and evaluation. Journal of Food Engineering, 215, 13-22.

Le Tohic, C., O'Sullivan, J. J., Drapala, K. P., Chartrin, V., Chan, T., Morrison, A. P., ... & Kelly, A. L. (2018). Effect of 3D printing on the structure and textural properties of pro-cessed cheese. Journal of Food Engineering, 220, 56-64.

Liu, W., Ye, A., Liu, W., Liu, C., & Singh, H. (2013). Stability during in vitro digestion of lactoferrin-loaded liposomes prepared from milk fat globule membrane-derived phospholipids. Journal of dairy science, 96(4), 2061-2070.

Lopez, C., Madec, M. N., & Jimenez-Flores, R. (2010). Lipid rafts in the bovine milk fat globule membrane revealed by the lateral segregation of phospholipids and heterogeneous distribution of glycoproteins. Food Chemistry, 120(1), 22-33.

Malone, E., & Lipson, H. (2007). Fab@ Home: the personal desktop fabricator kit. Rapid Prototyping Journal.

McClements, D. J. (2004). Protein-stabilized emulsions. Current opinion in colloid & interface science, 9(5), 305-313.

Michalski, M. C., Michel, F., Sainmont, D., & Briard, V. (2002a). Apparent ζ-potential as a tool to assess mechanical damages to the milk fat globule membrane. Colloids and Surfaces B: Biointerfaces, 23(1), 23-30.

Michalski, M. C., Cariou, R., Michel, F., & Garnier, C. (2002b). Native vs. damaged milk fat globules: membrane properties affect the viscoelasticity of milk gels. Journal of Dairy Science, 85(10), 2451-2461.

Michalski, M. C., Michel, F., & Geneste, C., (2002c). Appearance of submicronic particles in the milk fat globule size distribution upon mechanical treatments. Le Lait, 82(2), 193-208.

Mulder, H., & Walstra, P. (1974). The milk fat globule (p. 163). Farnham Royal: Commonwealth Agricultural Bureaux.

Nöbel, S., Seifert, B., Schäfer, J., Daffner, K., & Hinrichs, J. (2018). Oral presentation Food Colloids, Leeds 2018 - Session - Processing of Novel Structures for Functionality. Temperature-triggered gelation of milk concentrates applied to 3D food printing.

Nöbel, S., Seifert, B., Daffner, K., Schäfer, J., & Hinrichs, J. (2020). Instantaneous gelation of acid milk gels via customized temperature-time profiles: Screening of concentration and pH suitable for temperature triggered gelation towards 3D-printing. Food Hydrocolloids, 106450.

Ong, L., Dagastine, R. R., Kentish, S. E., & Gras, S. L., 2010a. The effect of milk processing on the microstructure of the milk fat globule and rennet induced gel observed using confocal laser scanning microscopy. Journal of food science, 75(3), E135-E145.

Ong, L., Dagastine, R. R., Kentish, S. E., & Gras, S. L. (2010b). Transmission electron microscopy imaging of the microstructure of milk in cheddar cheese production under different processing conditions. Australian Journal of Dairy Technology, 65(3), 222.

Rajagopalan, R., & Hiemenz, P. C. (1997). Principles of colloid and surface chemistry. Marcel Dekker, New-York, 8247, 8.

Roefs, P. F. M. (1986). Structure of acid casein gels: A study of gels formed after acidification in the cold (Doctoral dissertation, Roefs). Wageningen University & Research Centre.

Ross, M. M., Kelly, A. L., & Crowley, S. V. (2019). Potential Applications of Dairy Products, Ingredients and Formulations in 3D Printing. In Fundamentals of 3D Food Printing and Applications (pp. 175-206). Academic Press.

Schäfer, J., Läufle, I., Schmidt, C., Atamer, Z., Nöbel, S., Sonne, A., Kohlus, R. & Hinrichs, J. (2018). The sol−gel transition temperature of skim milk concentrated by microfiltration as affected by pH and protein content. International journal of dairy technology, 71(3), 585-592.

Sharma, S. K., & Dalgleish, D. G., (1993). Interactions between milk serum proteins and synthetic fat globule membrane during heating of homogenized whole milk. Journal of Agricultural and Food Chemistry, 41(9), 1407-1412.

Sharma, R., Singh, H., & Taylor, M. W. (1996a). Recombined milk: factors affecting the protein coverage and composition of fat globule surface layers. Australian journal of dairy technology, 51(1), 12.

Sharma, R., Singh, H., & Taylor, M. W. (1996b). Composition and structure of fat globule surface layers in recombined milk. Journal of Food Science, 61(1), 28-32.

Singh, H., & Creamer, L. K. (1991). Influence of concentration of milk solids on the dissociation of micellar κ-casein on heating reconstituted milk at 120° C. Journal of dairy research, 58(1), 99-105.

Van Vliet, T., & Dentener-Kikkert, A. (1982). Influence of the composition of the milk fat globule membrane in the rheological properties of acid milk gels. Netherlands Milk and Dairy Journal, 36, 261-265.

Van Vliet, T., 1988. Rheological properties of filled gels. Influence of filler matrix interaction. Colloid and Polymer Science, 266(6), 518-524.

Walstra, P., & Jenness, R. (1984). Dairy chemistry & physics. John Wiley & Sons. New York.

Walstra, P., Wouters, J. T. M., & Geurts, T. J. (2006). Dairy science and technology. Boca Raton, FL, USA: CRC Press.

Wegrzyn, T. F., Golding, M., & Archer, R. H. (2012). Food Layered Manufacture: A new process for constructing solid foods. Trends in Food Science & Technology, 27(2), 66-72.

Ye, A., Singh, H., Taylor, M. W., & Anema, S. (2002). Characterization of protein components of natural and heat-treated milk fat globule membranes. International Dairy Journal, 12(4), 393-402.

Ye, A., Anema, S. G., & Singh, H. (2008). Changes in the surface protein of the fat globules during homogenisation and heat treatment of concentrated milk. Journal of dairy research, 75(3), 347-353.

719 **Table Caption**

720 **Table 1.** Proportions of individual proteins covering the milk fat globule surface after thermal
721 (80°C, 10 min; pH adjusted to 6.55, 6.9 and 7.1) and mechanical treatment (sonication and
722 homogenisation).

723

724

725 **Figure Captions**

726 **Fig. 1.** Changes in the zeta-potential as a function of the pH of a micellar casein−whey protein
727 suspensions (8.0% (w/w) CS, 2.0% (w/w) WP) mixed with dairy fat (to 1.0% (w/w) total fat),
728 heated at pH 6.55 (●), at pH 6.9 (▲) and at pH 7.1 (Δ). For comparison, the zeta-potential of
729 non-heated micellar casein (○) without any fat is shown. The casein to whey protein ratio was
730 4:1.

731

732 **Fig. 2.** Particle size distribution of casein−whey protein suspensions mixed with different
733 amounts of fat to a total fat concentration of 1.0% (w/w), 2.5% (w/w) or 5.0% (w/w) after a
734 heating step at pH 6.55 (a), 6.9 (b) or 7.1 (c) with either no mechanical input (●/red) or soni-
735 cation/homogenisation at 500 bar (1.0% (w/w) fat = ◯/blue hollow circle; 2.5% (w/w) fat = ▲
736 /yellow triangle; 5.0% (w/w) fat = ■/green square). The inset graphs in all images focus on the
737 particle size distribution of each formulation between 1 – 1000 nm to better see differences as
738 a result of the addition of fat.

739 **Fig. 3.** CLSM micrographs of casein−whey protein suspensions mixed with milk fat (to a total
740 fat of 2.5% (w/w)) and then thermally (80°C, 10 min, pH 7.1) and mechanically (sonication +
741 homogenisation) treated. Samples were stained with FCF fast green and Nile red fluorescent
742 dyes (fat appears as red and protein as green) as seen on the left. The image after deconvolution
743 with Huygens software is shown on the right. The scale bars are each 5 μm in length.

744

745 **Fig. 4** Cryo-EM images of casein−whey protein (8.0% (w/w) CS and 2.0% (w/w) WP) suspen-
746 sions with 2.5 % (w/w) milk fat that have been thermally (80°C, 10 min; adjusted pH
747 6.55/6/9/7.1) and mechanically (sonication and homogenisation at 500 bar) treated. Samples
748 received a constant dose (5.72 e^{-}/Å s) but an increasing dose time (moving left to right across
749 the Figure, with the sample after the highest dosage appearing on the far right). A dilution of
750 1:10 with deionised water was used prior to analysis. The scale bar is 500 nm in length in all
751 images. The increasing contrast between protein and fat particles as a function of exposure was
752 used to differentiate between these two types of particles.

753

754 **Fig. 5.** SDS-PAGE analysis of proteins covering the milk fat globule surface membrane after
755 thermal (80°C, 10 min) and mechanical treatment. A total fat content of 2.5% (w/w) was ana-
756 lysed for each sample. The molecular weight ladder (kDa) is shown on the left; Lane I-II:
757 heated, pH 6.55; Lane III-IV: heated, pH 6.9; Lane V-VI: heated, pH 7.1.

758 **Fig. 6.** Sol−gel transition temperatures of cold acidified casein−whey protein suspensions
759 (8.0% (w/w) CS and 2.0% (w/w) WP) with different amounts of milk fat added (to final fat
760 contents of 1.0% (●), 2.5% (Δ), 5.0% (▲) and 0% (w/w) as comparison (○)) after heating at
761 pH 6.55 (A), 6.9 (B) and 7.1 (C) and cold acidified casein−whey protein suspensions (10.0%
762 (w/w) CS and 2.5% (w/w) WP) with different amounts of fat added after heating at pH 6.55
763 and 6.9 (D). A heating rate of 1 K min/min was applied.

764

765 **Fig. 7.** Aggregation rate (Pa/ 10K) of heated samples (80°C, 10 min, pH 6.55 (A), 6.9 (B) and
766 7.1 (C)) with constant protein content (8.0% (w/w) CS and 2.0% (w/w) WP) and with higher
767 protein content (10.0% (w/w) CS and 2.5% (w/w) WP, (D)) at different pH values (4.8 – 5.2)
768 with different amounts of fat added (to final fat contents of 1.0, 2.5 and 5.0% (w/w)) at 10°C
769 after/higher than sol−gel transition temperature obtained by temperature sweeps with a heating
770 rate of 1 K/min. The solid line in all images represents the aggregation rate of pure protein-
771 based formulations and is added to simplify comparisons to protein−fat suspensions. The dotted
772 line indicates the threshold where above 250 Pa/10 K the aggregation rate was used as a positive
773 indicator towards printability in a simple printing tests as shown by images of the printed sam-
774 ples.

775

776 **Fig. 8.** Schematic presentation depicting the preparation of casein−whey protein suspensions
777 mixed with milk fat for extrusion-based 3D-printing via the pH−T-route. After a thermal (80°C,
778 10 min, pH 6.55/ 6.9/ 7.1) and mechanical energy input, the newly created MFG membrane
779 surface is covered by different types of proteins or protein subunits/ aggregates.

780 **Supplementary Fig. 1.** Optical microscopy of a casein−whey protein suspension inclusive
781 added fat with native milk fat globules without any mechanical treatment (100x magnification).
782 Big particles all represent milk fat globules. Scale bar = 5 μm and 10 μm.

Figure 1

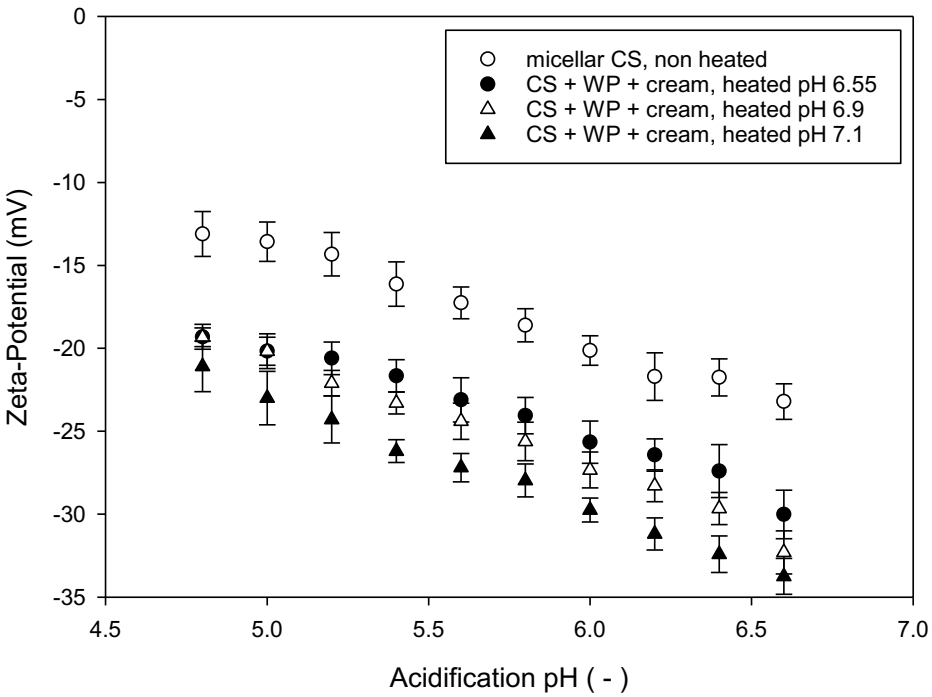
micellar CS, non heated
CS + WP + cream, heated pH 6.55
CS + WP + cream, heated pH 6.9
CS + WP + cream, heated pH 7.1
Zeta-Potential (mV)
0
-5
-10
-15
-20
-25
-30
-35
4.5
5.0
5.5
6.0
6.5
7.0
Acidification pH (-)

Figure 2

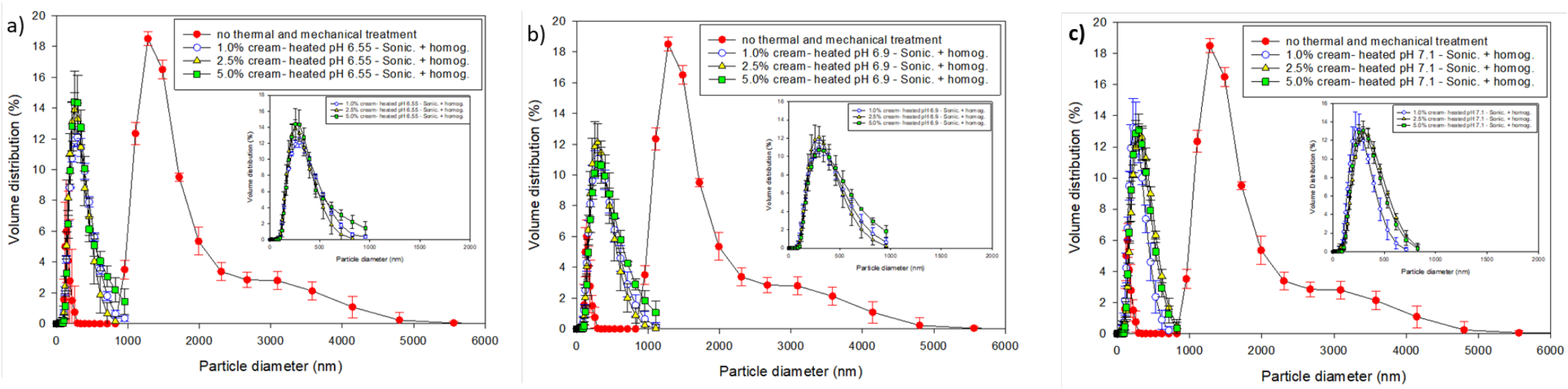
a)
no thermal and mechanical treatment
1.0% cream- heated pH 6.55 - Sonic. + homog.
2.5% cream- heated pH 6.55 - Sonic. + homog.
5.0% cream- heated pH 6.55 - Sonic. + homog.
Volume distribution (%)
Particle diameter (nm)
b)
no thermal and mechanical treatment
1.0% cream- heated pH 6.9 - Sonic. + homog.
2.5% cream- heated pH 6.9 - Sonic. + homog.
5.0% cream- heated pH 6.9 - Sonic. + homog.
Volume distribution (%)
Particle diameter (nm)
c)
no thermal and mechanical treatment
1.0% cream- heated pH 7.1 - Sonic. + homog.
2.5% cream- heated pH 7.1 - Sonic. + homog.
5.0% cream- heated pH 7.1 - Sonic. + homog.
Volume distribution (%)
Particle diameter (nm)

Figure 3

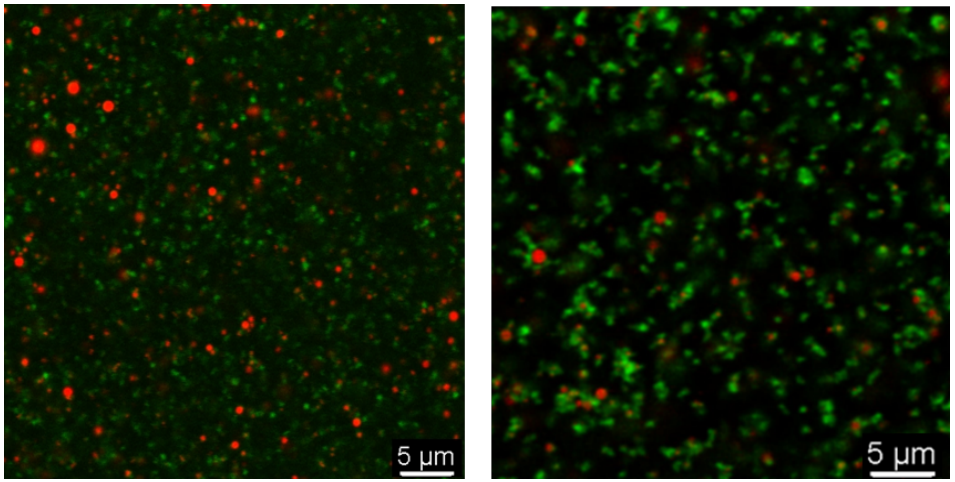

Figure 4

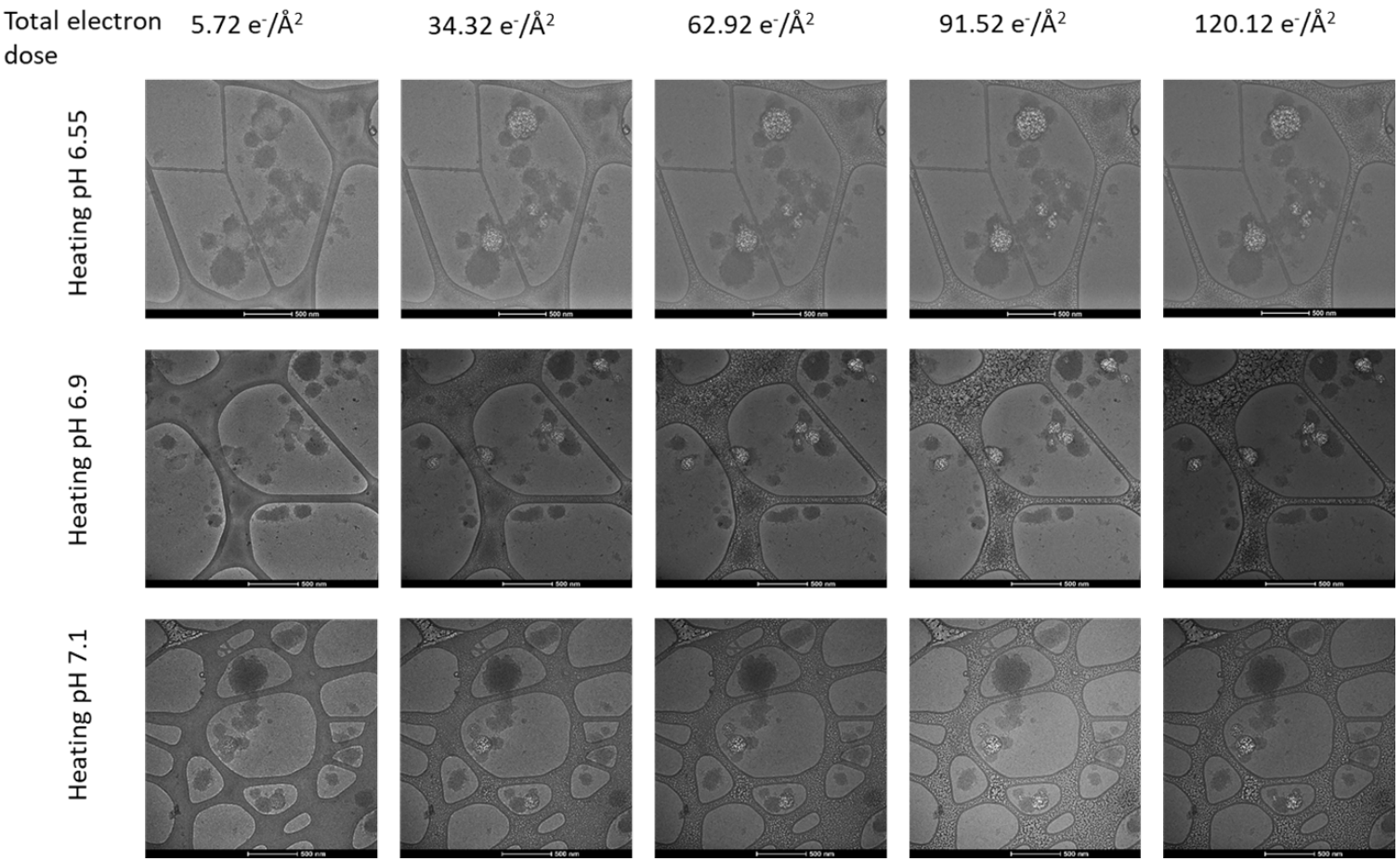
Total electron dose
5.72 e⁻/Å²
34.32 e⁻/Å²
62.92 e⁻/Å²
91.52 e⁻/Å²
120.12 e⁻/Å²
Heating pH 6.55
Heating pH 6.9
Heating pH 7.1

Figure 5

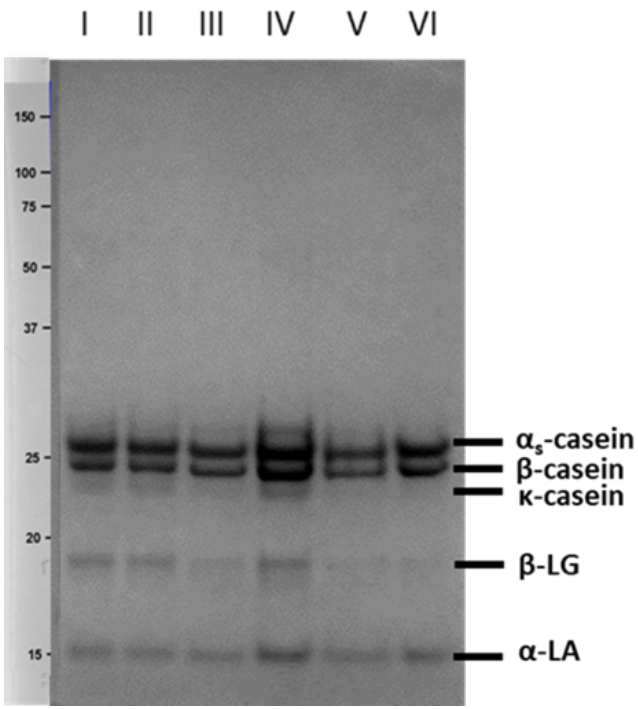
I
II
III
IV
V
VI
150
100
75
50
37
25
20
15
α_s-casein
β-casein
κ-casein
β-LG
α-LA

Figure 6

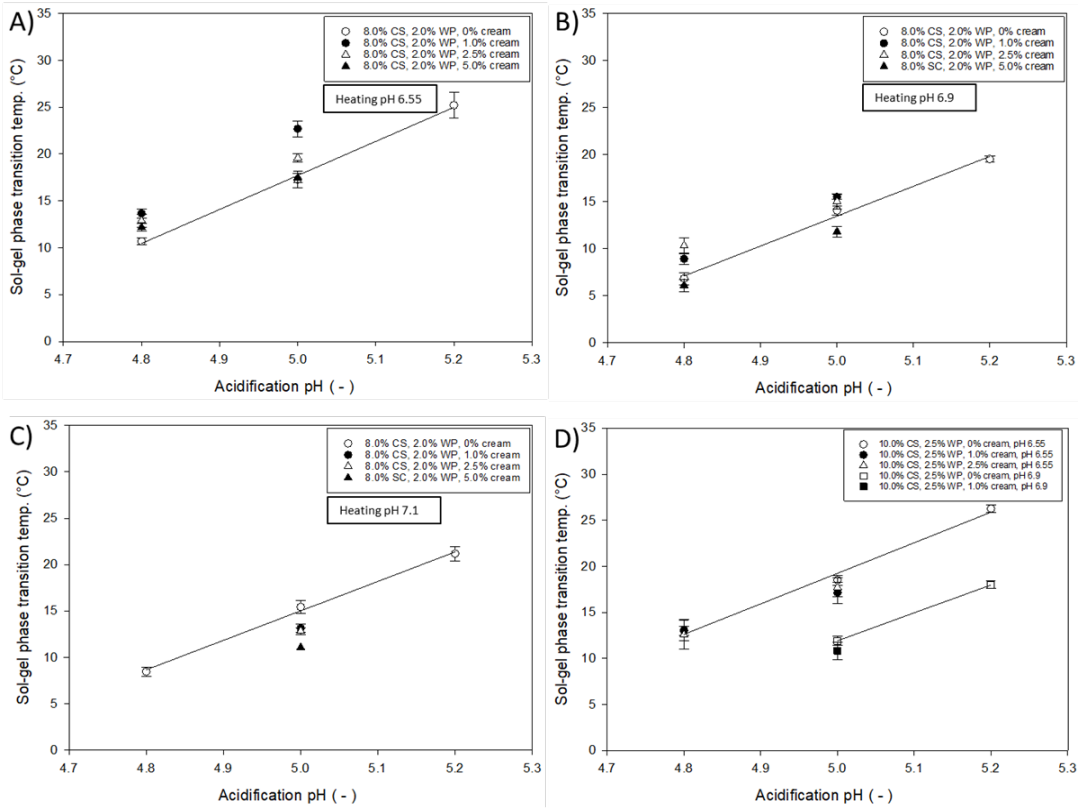
A)
8.0% CS, 2.0% WP, 0% cream
8.0% CS, 2.0% WP, 1.0% cream
8.0% CS, 2.0% WP, 2.5% cream
8.0% CS, 2.0% WP, 5.0% cream
Heating pH 6.55
Sol-gel phase transition temp. (°C)
Acidification pH (-)
B)
8.0% CS, 2.0% WP, 0% cream
8.0% CS, 2.0% WP, 1.0% cream
8.0% CS, 2.0% WP, 2.5% cream
8.0% SC, 2.0% WP, 5.0% cream
Heating pH 6.9
Sol-gel phase transition temp. (°C)
Acidification pH (-)
C)
8.0% CS, 2.0% WP, 0% cream
8.0% CS, 2.0% WP, 1.0% cream
8.0% CS, 2.0% WP, 2.5% cream
8.0% SC, 2.0% WP, 5.0% cream
Heating pH 7.1
Sol-gel phase transition temp. (°C)
Acidification pH (-)
D)
10.0% CS, 2.5% WP, 0% cream, pH 6.55
10.0% CS, 2.5% WP, 1.0% cream, pH 6.55
10.0% CS, 2.5% WP, 2.5% cream, pH 6.55
10.0% CS, 2.5% WP, 0% cream, pH 6.9
10.0% CS, 2.5% WP, 1.0% cream, pH 6.9
Sol-gel phase transition temp. (°C)
Acidification pH (-)

Figure 7

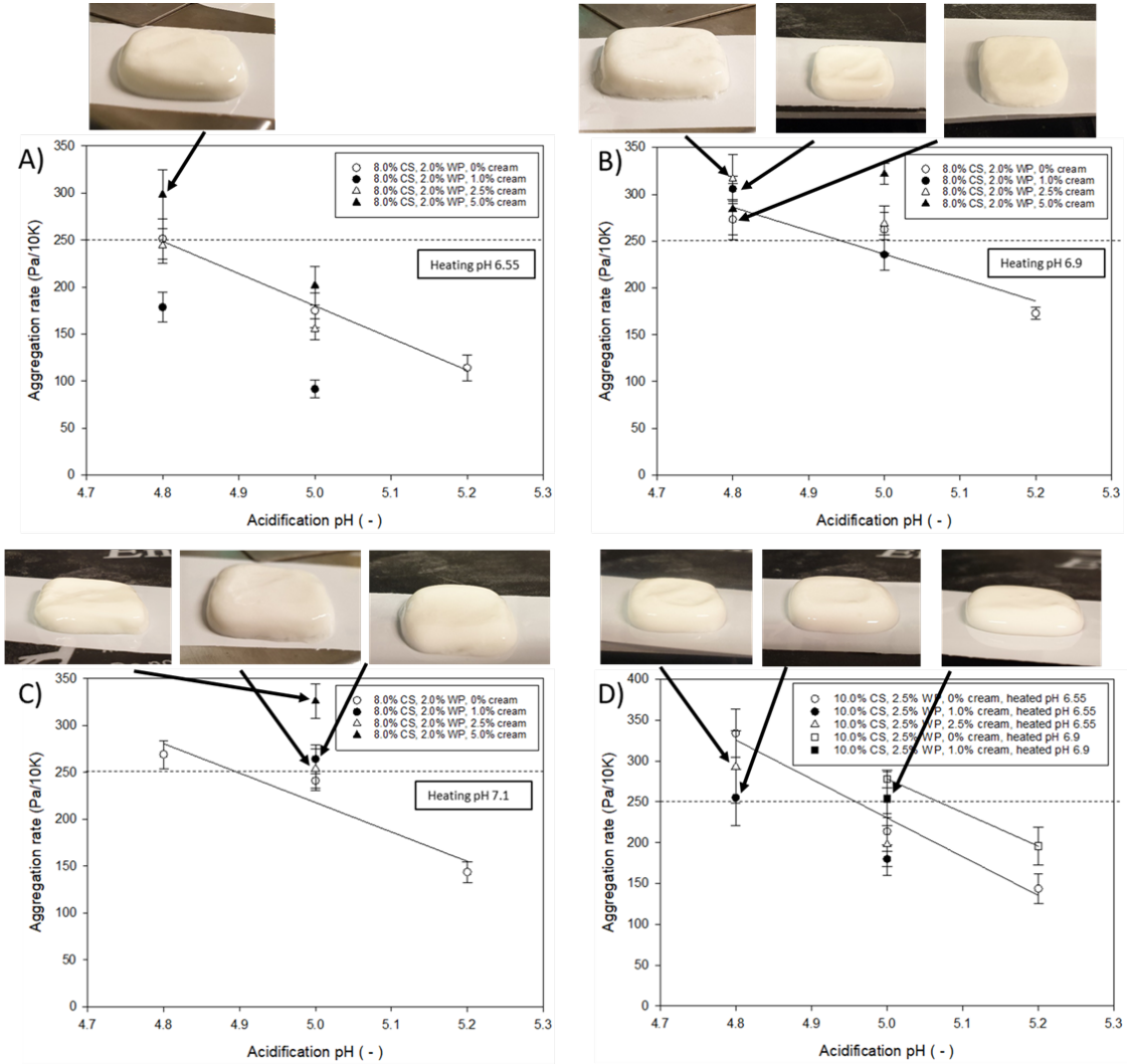
A)
8.0% CS, 2.0% WP, 0% cream
8.0% CS, 2.0% WP, 1.0% cream
8.0% CS, 2.0% WP, 2.5% cream
8.0% CS, 2.0% WP, 5.0% cream
Heating pH 6.55
Aggregation rate (Pa/10K)
Acidification pH (-)
B)
8.0% CS, 2.0% WP, 0% cream
8.0% CS, 2.0% WP, 1.0% cream
8.0% CS, 2.0% WP, 2.5% cream
8.0% CS, 2.0% WP, 5.0% cream
Heating pH 6.9
Aggregation rate (Pa/10K)
Acidification pH (-)
C)
8.0% CS, 2.0% WP, 0% cream
8.0% CS, 2.0% WP, 1.0% cream
8.0% CS, 2.0% WP, 2.5% cream
8.0% CS, 2.0% WP, 5.0% cream
Heating pH 7.1
Aggregation rate (Pa/10K)
Acidification pH (-)
D)
10.0% CS, 2.5% WP, 0% cream, heated pH 6.55
10.0% CS, 2.5% WP, 1.0% cream, heated pH 6.55
10.0% CS, 2.5% WP, 2.5% cream, heated pH 6.55
10.0% CS, 2.5% WP, 0% cream, heated pH 6.9
10.0% CS, 2.5% WP, 1.0% cream, heated pH 6.9
Aggregation rate (Pa/10K)
Acidification pH (-)

Figure 8

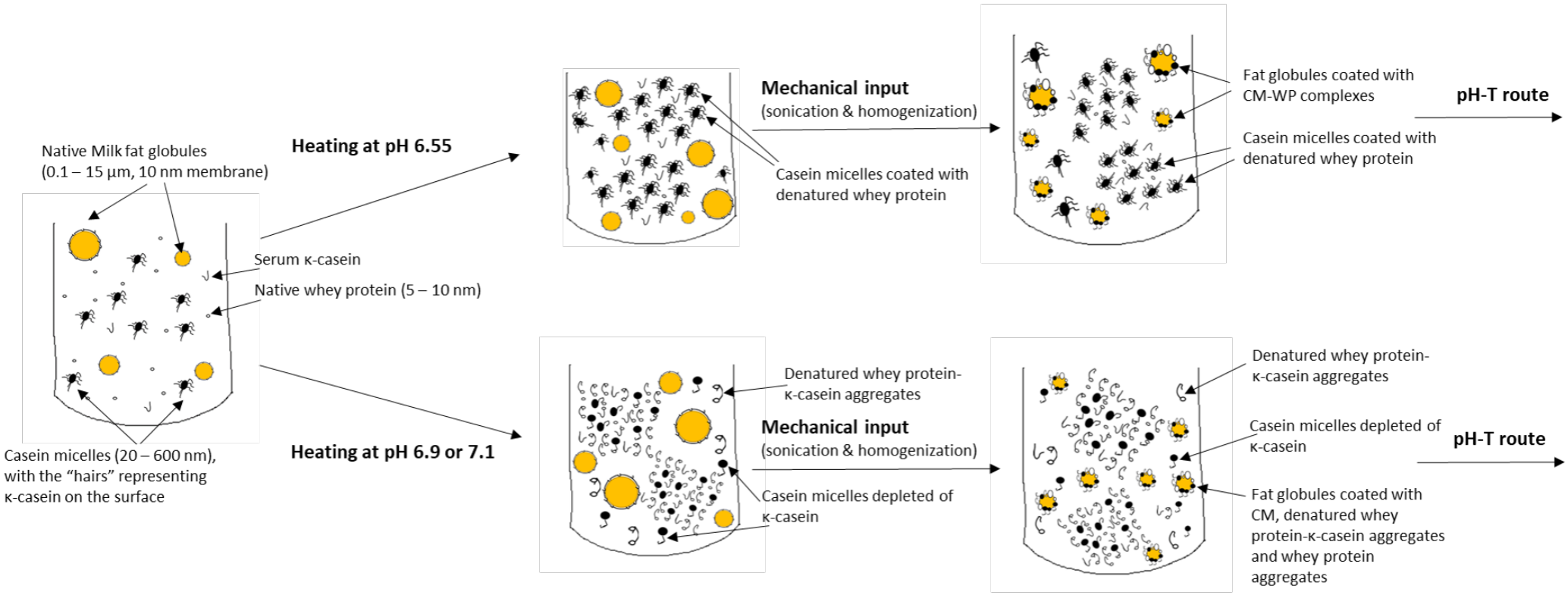
Native Milk fat globules
(0.1 – 15 µm, 10 nm membrane)
Serum κ-casein
Native whey protein (5 – 10 nm)
Casein micelles (20 – 600 nm), with the "hairs" representing κ-casein on the surface
Heating at pH 6.55
Heating at pH 6.9 or 7.1
Mechanical input
(sonication & homogenization)
Casein micelles coated with denatured whey protein
Fat globules coated with CM-WP complexes
Casein micelles coated with denatured whey protein
pH-T route
Denatured whey protein-κ-casein aggregates
Mechanical input
(sonication & homogenization)
Casein micelles depleted of κ-casein
Denatured whey protein-κ-casein aggregates
Casein micelles depleted of κ-casein
Fat globules coated with CM, denatured whey protein-κ-casein aggregates and whey protein aggregates
pH-T route